# Impact of various drying technologies on the drying characteristics, physicochemical properties, and antioxidant capacity of walnut green husk

**Jingfang Ao**
Northwest A&F University
**Jun Wang**
Northwest A&F University
**Heyu Shen**
Northwest A&F University
**Yongkang Xie**
Henan Academy of Agricultural Sciences
**Yingying Cai**
Northwest A&F University
**Meihua Xi**
Northwest A&F University
**Yujie Hou**
Northwest A&F University
**Mei Li**
Northwest A&F University
**Anwei Luo** ( luoanwei@nwsuaf.edu.cn )
Northwest A&F University

**Research Article**

**Keywords:** walnut green husk, drying, bioactive compounds, specific energy consumption, microstructure

**Posted Date:** October 12th, 2023

**DOI:** https://doi.org/10.21203/rs.3.rs-3415065/v1



**Additional Declarations:** No competing interests reported.

# Impact of various drying technologies on the drying characteristics, physicochemical properties, and antioxidant capacity of walnut green husk

Jingfang Ao[a1], Jun Wang[a1], Heyu Shen[a], Yongkang Xie[b], Yingying Cai[a], Meihua Xi[a], Yujie Hou[a], Mei Li[a], Anwei Luo[a*]

*a College of Food Science and Engineering, Northwest A&F University, Yangling, 712100, China*

*b Henan Academy of Agricultural Sciences, Zhengzhou, 450002, China*

*Correspondence: Anwei Luo, College of Food Science and Engineering, Northwest A&F University, Yangling, Shaanxi 712100, China.

Email: 2637563894@qq.com (Jingfang Ao), jun.wang@nwafu.edu.cn (Jun Wang), luoanwei@nwsuaf.edu.cn (Anwei Luo[a*]).

Orcid ID: 0000-0001-9505-0729 (Anwei Luo[a*])

[1] these authors contributed equally to this work and should be considered co-first authors.

**Authors' Contributions**

Jingfang Ao: Methodology, Investigation, Data curation, Formal analysis Writing-Original draft preparation; Jun Wang: Reviewing and Editing; Heyu Shen: Methodology, Data curation, Software; Yongkang Xie: Reviewing and Editing; Yingying Cai: Investigation, Data curation; Meihua Xi: Reviewing; Yujie Hou: Reviewing; Mei Li: Reviewing and Editing; Anwei Luo*: Writing- Reviewing and Editing.

**Funding**

We gratefully acknowledge the financial support from the National Key R&D Program of China (2019YFD1002404).

**Data Availability Statement**

The datasets generated or analyzed during this study areavailable from the corresponding author on reasonable request.

## Abstract

Walnut green husk (WGH) is common agricultural by-product with high yield and serious pollution. The present study aimed to evaluate the impacts of solar drying (SD), pulsed vacuum drying (PVD), short and medium infrared radiation drying (SMIR), hot air drying based on temperature and humidity control (TH-HAD), and heat pump drying (HPD) on the drying characteristics, energy consumption, physicochemical properties, bioactive compounds content and antioxidant capacity of WGH. Drying characteristics and drying kinetics showed that artificial drying can significantly improve drying efficiency. Compared with SD, the drying time of PVD, SMIR, TH-HAD, and HPD were reduced by 63.57%, 78.68%, 66.28%, and 53.97%, respectively. Specific energy consumption analysis demonstrated that HPD showed the lowest specific energy consumption, 2.15 kW·h/kg. Hydration properties analysis revealed PVD had the best water holding capacity and HPD sample had the best water solubility index (43.44%). Structural analysis showed the cell wall structure of WGH was damaged by different drying methods. Overall, Among the five drying methods, HPD has lower energy consumption, less time, and maintains good antioxidant activity. HPD has good potential in the commercial-scale production of WGH.

**Keywords:** walnut green husk; drying; bioactive compounds; specific energy consumption; microstructure

## 1 Introduction

Walnut (*Juglans regia* L.) is one of the most important and valuable agricultural products worldwide. With an emphasis on vigorous promotion of the woody oil industry, the walnut industry has rapid growth. Particularly, China is the greatest Asia producer of walnuts. According to the Food and Agriculture Organization (FAO), China's walnut production reached $1.1 \times 10^6$ tonnes in 2020, accounting for about one-third of the world's total walnut production (FAO, 2020). Walnut green husk

(WGH) is the major by-product of walnut processing, representing around 50-60% (w/w) of the total walnuts (Asgari et al., 2020). Therefore, China generates approximately 550,000 tonnes of WGH annually. However, WGH is not fully used, and most of them are discarded as waste, rapidly decaying and causing environmental pollution. Moreover, WGH is a relevant source of bioactive compounds, such as polyphenols, flavonoids, terpenoids, naphthoquinones, and pectins (Romano et al., 2021), which can be used as an antioxidant and antibacterial agent in the food industry and have been used on the preservation of fresh-cut apple and rainbow trout during refrigerated storage (Mozaffari et al., 2022; Jiang et al., 2022) WGH extract is also able to inhibit the activity of α -glucosidase, thus regulating human blood sugar levels. Additionally, the WGH is conducive to the phytoremediation of heavy metals due to the presence of phenolic hydroxyl, carboxyl, and other functional groups (Liu et al., 2022).

However, the fresh WGH has a high moisture content (about 90%) and strong biological activity, promoting the growth of microorganisms and accelerating the decay rate, resulting in mildew and rot, which is not conducive to subsequent processing and utilization. Therefore, exploring an energy-saving drying technology for WGH is extremely important for industrial applications. The current drying technology in industrial production includes solar drying (SD) and artificial drying. The advantage of SD is that it does not require any mechanical power or energy consumption. Nonetheless, SD has several disadvantages, including long drying time, overheating caused by direct exposure, and nonuniform shrinkage of the product due to inclement weather, resulting in a product with poor quality and a high possibility of contamination (Adenitan et al., 2021). Common artificial drying methods in agricultural product processing include pulsed vacuum drying (PVD), short and medium infrared radiation drying (SMIR), hot air drying based on temperature and humidity control (TH-

HAD), and heat pump drying (HPD). PVD and SMIR use innovative heating units to reduce energy consumption and improve drying uniformity. Recently, Xie et al. (2017) used PVD to process blueberries and obtained better quality. TH-HAD improves product quality by adjusting the drying temperature and the relative humidity of the drying medium, which is an improvement on traditional hot air drying. Additionally, one study developed an ultrasound pretreatment combined with and hot-air drying technique for sweet potatoes (Tayyab Rashid et al., 2022). The authors found that this combination could save energy and improve textural qualities (hardness and resilience). HPD recycles the sensible and latent heat in the exhaust gas during drying, reducing energy consumption. It is the most suitable new environmental-friendly and energy-saving drying method to replace traditional drying at this stage and has been employed in the drying of kelp (Zhang et al., 2022).

This study aimed to solve the problems of pollution, perishability, and difficulty in preserving WGH. Five drying methods (SD, PVD, SMIR, TH-HAD, and HPD) are used to dry WGH, and the effects of different drying methods on the drying characteristics, energy consumption, physicochemical properties, bioactive compounds content, and antioxidant capacity were compared, so as to screen out an energy-saving and efficient drying method suitable for WGH. The results of this study could provide technical support for WGH from ground to industrial production and supply a raw material reserved for further development and utilization of WGH.

## 2. Materials and methods

### *2.1. Materials*

The fresh WGH samples (Xiangling variety) were collected from Huairou Market in Beijing. The collected samples were transported back to the laboratory within 5 hours, and their initial

moisture content (about 90%, w.b.) was measured using a moisture meter (HDS-16, Fangrui Instrument Co., Ltd., Shanghai, China), and then the drying experiment was carried out to prevent it from corrupting and deteriorating.

### *2.2. Drying methods*

The clean fresh WGH was dried using five drying methods and then pulverized to 40 mesh for use. For SD, a single layer of fresh WGH was placed on the ground and covered with gauze to protect against mosquitoes. It was exposed to sunlight for about 8 hours daily until the moisture content of the WGH was less than 10% on a wet basis.

For artificial drying methods (PVD, SMIR, TH-HAD, and HPD), the WGH was placed on the tray in the drying chamber with a load of about 25 kg/m$^2$ and set according to the parameters described in Table 1. In general, the higher the drying temperature, the shorter the drying time and the lower the drying cost. But a high drying temperature will cause damage to the active substances in the sample. Therefore, based on the previous experiments, the drying temperature of WGH was defined as 65 ◦C. During the drying process, the sample tray was taken out every 30 min, weighed, and placed back into the chamber. Drying was continued until the weight change of samples within 0.1 g on two consecutive weighings. Each treatment was performed in triplicate.

### *2.3. Drying characteristics*

The moisture ratio (MR) of WGH during drying experiments was calculated using the equation Eq.1:

$$\mathrm{MR}=\frac{M_t-M_e}{M_0-M_e} \quad (1)$$

Where, $M_t$ is the moisture content of WGH at time $t$ during the drying process, $M_0$ and $M_e$ are

the initial and equilibrium moisture content, respectively. All moisture contents was expressed on a dry basis (d.b.).

The value of the $M_e$ was much smaller than $M_t$ and $M_0$. Thus, Eq.1 can be simplified to Eq.2:

$$MR=\frac{M_t}{M_0} \tag{2}$$

The drying rate (DR) at a given time of WGH during various drying processes was computed according to Eq.3:

$$DR=\frac{M_{t_1}-M_{t_2}}{t_2-t_1} \tag{3}$$

Where, $t_1$ and $t_2$ are the drying times in minutes, $M_{t_1}$ and $M_{t_2}$ corresponds to the moisture contents of WGH at time $t_1$ and $t_2$ (g/g, dry basis).

### *2.4. Drying kinetics modeling*

Five currently used thin-layer drying models of agricultural products were used to fit the model to the optimal segmented pulsed vacuum drying method and used to further predict drying characteristics (An et al., 2019; Tunckal and Doymaz, 2020). The expressions of each drying kinetic model are as follows (Eq.4-Eq.8):

$$\text{Page model: } MR = e^{(-kt^n)} \tag{4}$$

$$\text{Henderson-Pabis model: } MR = ae^{(-kt)} \tag{5}$$

$$\text{Wang-Singh model: } MR = a+bt+ct^2 \tag{6}$$

$$\text{Lewis model: } MR = e^{(-at)} \tag{7}$$

$$\text{Logarithmic model: } MR = a+be^{(-kt)} \tag{8}$$

Where, k, n, a, b, c are the respective model parameters and t is the drying time.

The simplified chi-square ($\chi^2$), correlation coefficient ($R^2$), root mean square error (RMSE), and

residual sum of squares (RSS) between predicted and experimental values were applied to assess the model fit results.

$$\chi^2=\frac{\sum_{i=1}^{N}(A_{pre,i}-A_{exp,i})}{N-z} \tag{9}$$

$$R^2=1-\frac{\sum_{i=1}^{N}(A_{pre,i}-A_{exp,i})^2}{\sum_{i=1}^{N}(\overline{A_{pre,i}}-A_{exp,i})^2} \tag{10}$$

$$RMSE=\left[\frac{1}{N}\sum_{i=1}^{N}(A_{pre,i}-A_{exp,i})^2\right]^{\frac{1}{2}} \tag{11}$$

$$RSS=\sum_{i=1}^{N}(A_{pre,i}-A_{exp,i})^2 \tag{12}$$

where $A_{exp,i}$ and $A_{pre,i}$ are the experimental and predicted values, respectively, N is the total number of moisture ratios recorded in the experiment and z is the number of parameters in the model.

### *2.5. Specific energy consumption*

The specific energy consumption (SEC) indicates the sample's water content that can be removed per unit of energy consumption, and it is essential to evaluate the efficiency of the different drying methods. In this study, SEC was calculated by Eq.13 during all artificial drying processes :

$$SEC = \frac{W}{M} \tag{13}$$

Where, $W$ is the power consumption (kW·h) obtained from an electric meter, and $M$ is the loss of water removed during drying (kg).

### *2.6. Analysis of physical properties and structure*

#### *2.6.1. Hydration properties determination*

The determination of water holding capacity (WHC) and water solubility index (WSI) were adjusted using a previous methodology (Deli et al., 2019). Briefly, 3 g of WGH powder was weighed ($M_d$) into a conical flask, and water was added to disperse the powder with a water/powder ratio of

15 (w/w). Then the mixture was stirred and centrifuged. The mass of the sediment in the centrifuge tube was denoted as $M_W$, the supernatant was placed in an aluminum box ($S_0$), and the weight after drying to constant weight was denoted as $S_1$. WHC and WSI were calculated using Eq.14 and Eq.15:

$$\text{WHC}\ (\%)=\frac{(M_w\text{-}M_d)}{M_d}\times 100\ \% \tag{14}$$

$$\text{WSI}\ (\%)=\frac{(S_1\text{-}S_0)}{M_d}\times 100\ \% \tag{15}$$

*2.6.2. Color measurement*

The color parameter of the dried walnut green peel husk powder was measured by spectrophotometer (CS-820, Hangzhou Caipu Technology Co., Ltd, China) according to the CIE-Lab color system. The $L^*$ refers to the lightness index, ranging from 0 (darkness) to 100 (whiteness). $a^*$ and $b^*$ are chromaticity index, representing greenness (-)/redness (+) and blueness (-)/yellowness (+), respectively. The total color difference ($\Delta E$) between the dried and the fresh samples, chroma ($C$), and hue angle ($H^0$) was calculated using the equations Eq.16-Eq.18. The value of $H^0$ varies from 0° to 360°, indicating the change of the sample color from pure red to pure green (Seerangurayar. et al., 2019).

$$\Delta E=\sqrt{\left(L_0^*\text{-}L^*\right)^2+\left(a_0^*\text{-}a^*\right)^2+\left(b_0^*\text{-}b^*\right)^2} \tag{16}$$

$$C=\sqrt{(a^*)^2+(b^*)^2} \tag{17}$$

$$H^0=\tan^{-1}\left(\frac{b^*}{a^*}\right) \tag{18}$$

Where $L_0^*$, $a_0^*$, and $b_0^*$ were measured from the fresh WGH. $L^*$, $a^*$, and $b^*$ are the color parameters of the dried WGH samples.

*2.6.3. Microstructure by scanning electron microscope (SEM)*

A scanning electron microscope (Nova Nano SEM 450, FEI Co., Czech Republic) was used to observe the cross-sectional of dried WGH and to analyze microstructure changes. After being sprayed

with gold, the samples were observed under the microscope at the magnification of 800 with a 5.0 kV accelerating voltage.

*2.6.4. Fourier-transform infrared spectroscopy (FTIR)*

The WGH powder was analyzed by FTIR containing vetex 70 Fourier infrared spectrometer (Bruker, Karlsruhe, Germany). Briefly, the WGH powder (2 mg) treated with different drying methods was mixed with KBr (300 mg). After being pressed into slices, the scanning analysis was performed in the wavelength range of 4000 $cm^{-1}$ to 400 $cm^{-1}$ (Sarkar, 2021). The infrared spectrum baseline needed to be corrected and output as a DPT file.

### *2.7. Extraction and Analysis of bioactive substances of WGH*

The preparation of walnut green husk extract (WGHE) was performed according to a previous described methodology (Shen et al., 2022). Briefly, the dried WGH powder with a crushing degree of 40 mesh and 75% ethanol solution was mixed at a liquid-solid ratio of 1:50 (w/v), followed by an ultrasonically extraction in the ultrasonic power of 490 W and ultrasonic temperature of 60 ˚C for 140 min. The extracts were centrifuged at 7000 rpm for 15 min and the supernatant was collected. The supernatant was concentrated and dissolved in methanol as WGHE.

*2.7.1. Determination of bioactive compounds content*

The total phenolic content (TPC) in WGH was determined by the Folinol colorimetry, and the absorbance was measured at 760 nm (Xiang et al., 2019). The total flavonoid content (TFC) and total terpenoid content (TTC) in WGH were determined by the $NaNO_2$-$Al(NO_2)_3$ method (Tu et al., 2018) and Vanillin-Glacial acetic acid method (Shen et al., 2022). Rutin and Oleanolic acid were used as standards, respectively. Finally, the TFC and TTC were calculated based on the calibration curves of

rutin ($Y = 7.6124x + 0.0897$, $R^2 = 0.9995$) and oleanolic acid ($Y = 3.7774x + 0.0884$, $R^2 = 0.9997$). The determination of quinone content (QC) in WGH was carried out with spectrophotometry (Qin et al., 2022). The results were shown in Juglone equivalent (mg JE/g DM).

*2.7.2. High-resolution liquid chromatography-mass spectrometry (HRLCMS) profiling and analysis*

A high-resolution liquid chromatography-mass spectrometry (HRLCMS) was used to detect the phenolic components in the WGHE. An ultra-high performance liquid chromatography tandem with a high-resolution tandem quadrupole mass spectrometer system (Triple TOF® 5600+, AB Sciex, Singapore) equipped with an electrospray Ionization (ESI) and a Shim-pack Velox SP-C18 column (150 mm × 2.1 mm, 2.7 μm) was used for this assay. The elution was performed using solvent A (0.1% formic acid in water) and solvent B (acetonitrile) at a flow rate of 300 μL/min. The gradient elution program was optimized as follows: 0-10 min, 5%-8%B; 10-20 min, 8%-16.5%B; 20-28 min, 16.5%-22%B; 28-33 min, 22%-27%B; 33-38 min, 27%-30%B; 38-45 min, 30%-40%B; 45-50 min, 40%-50%B; 50-53 min, 50%-95%B; 53-55 min, 95%-5%B. The injection volume was 10 μL, and the column temperature was 40 °C. Finally, data acquisition and processing were performed using Analyst TF 1.7.1kit, PeakView2.2, MasterView and MultiQuant 3.0.2.

### *2.8. Evaluation of antioxidant activity*

*2.8.1. DPPH radical scavenging activity*

The free radical scavenging ability of WGHE was determined by the 2, 2-Diphenyl-1-picrylhydrazyl (DPPH) free radical scavenging method (Bettaieb Rebey et al., 2020). The absorbance was obtained at 517 nm by an enzyme labeling instrument and the results were expressed as a percentage of DPPH radical scavenging and calculated according to the equation Eq.19:

$$\text{DPPH scavenging rate (\%)} = \left[1 - \frac{(A_1 - A_2)}{A_0}\right] \times 100 \quad (19)$$

Where $A_0$, $A_1$, and $A_2$ are the absorbance of the control without the sample, the sample, and the sample without DPPH, respectively.

*2.8.2. ABTS radical scavenging activity*

ABTS radical scavenging activity was determined using a previous method with slight modifications (Nguyen et al., 2015). Briefly, the WGHE (1 mL) was mixed with 5 mL ABTS working solution, and the mixture was incubated in the dark at room temperature for 30 min. Then, the absorbance was measured at 734 nm. The results were calculated with the Eq.20:

$$\text{ABTS scavenging rate (\%)} = \left[1 - \frac{(A_2 - A_1)}{A_0}\right] \times 100 \quad (20)$$

Where $A_0$, $A_1$, and $A_2$ are the absorbance of the control without the sample, the sample, and the sample without ABTS solution, respectively.

*2.8.3. ·OH radical scavenging activity*

·OH radical scavenging activity was determined by a previous methodology according to Zheng et al (2015). The absorbance was measured at 510 nm. In this assay, ascorbic acid was used as a positive control. The ·OH radical scavenging rate was calculated using the equation Eq.21:

$$\text{·OH scavenging rate (\%)} = \left[1 - \frac{(A_1 - A_2)}{A_0}\right] \times 100 \quad (21)$$

Where, $A_0$, $A_1$, and $A_2$ are the absorbance of the control without the sample, the sample, and the sample without ferrous sulfate solution, respectively.

*2.8.4. Ferric reduction antioxidant power*

The antioxidant capacity of WGHE was determined by the modified ferric reduction antioxidant power (FRAP) (Ozsoy et al., 2008). Briefly, a mixture of 1 mL WGHE, 2.5 mL potassium ferricyanide (1%), and 2.5 mL phosphate buffer (pH 6.6) was added to the test tube for 20 min, after the reaction,

trichloroacetic acid (10%) was added and centrifuged at 8000 rpm for 5 min. Then, the absorbance of the extract was measured at 700 nm after mixing supernatant with ferric chloride (0.1%).

### *2.10. Statistical analysis*

All the experiments were carried out in triplicate, and the data were presented as mean ± standard deviation. The SPSS statistical software (version 20.0) was used to perform statistical analysis (ANOVA and Duncan multiple range test). The statistical significance of the differences was tested at the 95% probability level ($P < 0.05$). In addition, the principal component analysis (PCA) and clustering heat map analysis was used to analyze the bioactive substances, antioxidant activity, drying time, and specific energy consumption of WGH with five different drying methods.

## 3 Results and discussion

### *3.1. Drying characteristics analysis*

The drying curves of WGH are shown in Fig. 1A. The moisture ratio of WGH decreased with the increase of drying time under different drying methods. Compared with SD, PVD, SMIR, TH-HAD and HPD reduced the drying time of WGH to the same water content by 63.57%, 78.68%, 66.28%, and 53.97%, respectively, indicating that artificial drying can significantly improve drying efficiency. This was in agreement with the findings of Singh Sonia et al., (2021) that artificial drying can greatly reduce the drying time.

The drying rates of WGH under different drying methods (Fig. 1B) showed that the drying stages of SMIR and PVD mainly showed a deceleration period, in which the drying rate of SMIR decreased significantly while that of PVD decreased gently. PVD showed two short constant rate periods at the

moisture content of 0.77-1.00 g/g (d.b.) and 0.26-0.38 g/g (d.b.). TH-HAD and HPD first showed a period of acceleration, followed by a sharp downward trend. The fluctuation of HPD at the early stage of drying (when the moisture content was greater than 0.91 g/g on a dry basis) might be due to the instability of the pre-drying system. The results indicated that the diffusion of internal moisture dominated the drying process during the drying of WGH (Xu et al., 2020).

### *3.2. Drying kinetics modeling analysis*

Predicting and optimizing the performance of thin-layer drying models is essential in order to successfully transfer the results of experimental studies to industrial-scale operations (Benseddik et al., 2018). The moisture content data were fitted to five thin-layer drying models and the results of the statistical analysis were shown in Table 2. The best-suited model selected based on the highest $R^2$, the lowest $\chi^2$, RMSE, and RSS (Deng et al., 2020). In comparison with other models, Wang-Singh model was found to be the most suitable for TH-HAD ($R^2$ = 0.9972) and HPD ($R^2$ = 0.9984) drying data of WGH. The optimum drying models for PVD and SMIR of WGH were Page model ($R^2$ = 0.9997) and Logarithmic model ($R^2$ = 0.9975), respectively.

### *3.3. Specific energy consumption analysis*

Drying is one of the high energy-consuming links in industrial production. A green and energy-saving drying method can not only save production costs but also meet the market demand, so it is especially important to take energy consumption as the most important reference index when evaluating the drying process. The specific energy consumption (SEC) values for different drying methods of WGH are shown in Fig. 1A. The results of the correlation analysis (Fig. 5) showed that the drying time showed a significant correlation with the energy consumption ($p<0.01$). These results

were similar to a previous study performed with Okra (Ismail et al., 2019). However, it is interesting to note that HPD had the longest drying time but the lowest energy consumption (2.15 kW·h/kg). This may be due to the fact that the HPD system requires only the energy input of the heat pump compressor, while its exhaust waste heat can be recovered by the system evaporator, improving the system efficiency ratio (Onwude et al., 2018).

### *3.4. Physical properties and structural analysis*

#### *3.4.1. Hydration properties*

The hydration properties are related to the density, exposure of hydrophilic groups and microstructure of the samples (Hu et al., 2013). Table 3 showed the WHC and WSI values of WGH powder obtained by different drying methods. The order of WHC values is: PVD > TH-HAD > SMIR > SD > HPD, probably due to the fact that PVD has less damage to the internal tissue of WGH during the drying process and the structure is more compact. The highest WSI values of HPD samples were probably due to the formation of neat honeycomb porous structure inside the samples during the drying process, which damaged the internal tissues of WGH more severely and leached more soluble substances than other drying methods. The lowest WSI value of the PVD samples was different from the results of previous studies (Xu et al., 2021), which might be due to the sample variability, as the WGH was thicker and the water channels were not completely opened in PVD, resulting in less soluble substances leaching.

#### *3.4.2. Color characteristics*

The color parameters $L^*$, $a^*$, $b^*$, $\Delta E$, $C$, and $H^0$ values of walnut green bark under different drying conditions were shown in Table 4. The brightness of fresh WGH ($L^*$=56.83) was significantly higher

than that of the dried treated ones. For the dried WGH, the highest $L^*$ values were found for the PVD and HPD samples, indicating that the samples had higher brightness and luminosity, which may be due to the pulsed vacuum environment of PVD and the drying process of HPD may reduce the occurrence of browning (Xie et al., 2017). The $b^*$ values of the samples were influenced by the drying methods and these color changes in yellowness are probably related to the browning reaction due to drying (Senadeera et al., 2020). There were no significant differences ($p<0.05$) in $a^*$ values among dried WGH samples. The total color difference ($\Delta E$) was commonly used to assess the differences between dried and fresh samples (Deng et al., 2019). The $\Delta E$ values of the dried samples were all greater than 5, indicating that drying significantly affects the color. $C$ values represents the purity or saturation and the TH-HAD samples showed higher $C$ values than other drying methods, indicating a bright surface color. An orange-red color was observed when $H^0 < 90$, and the lower the value of $H^0$, the deeper the red-orange observed. It can be seen that the $H^0$ value of SD is significantly lower than that of the artificial drying methods, which may be caused by the longer SD time of WGH.

*3.4.3. Microstructure*

To explain the differences in the hydration characteristics of WGH after different drying methods at the microscopic level, the microstructure of WGH was further observed by scanning electron microscopy (Fig. 2). It could be seen that the microstructure of WGH was significantly different under different drying methods. The HPD samples (Fig. 2E) had a neat honeycomb porous structure with a larger surface porosity, which facilitated the entry of water, making the water solubility index higher (Namsanguan et al., 2004). The enlarged and connected pores of the SD (Fig. 2A) and SMIR (Fig. 2C) samples facilitated water transfer. The TH-HAD (Fig. 2D) and PVD (Fig. 2B) samples had less pore structure, resulting in a lower water solubility index of WGH. These SEM

observations are consistent with the analysis of the hydration properties of samples and confirm the hypothesis of the causes for the differences in the hydration properties of the dried WGH.

*3.4.4. Fourier-transform infrared spectroscopy*

The Fourier transform infrared spectra of the different WGH powder samples that with different drying methods were displayed in Fig. 3. All samples showed peak-like bands in position and shape, but differed in peak intensity. The peak absorption intensity by artificial drying was significantly enhanced, indicating that the interaction among the hydrogen-bonded components was destroyed (Lugo-Lugo et al., 2017). The band at 3361 $cm^{-1}$ was recognized as O-H telescopic vibration. The absorption peak at 2922 $cm^{-1}$ corresponds to the absorption of the C-H stretching vibration on pyran. The characteristic peaks at 1728 $cm^{-1}$, 1610 $cm^{-1}$ and 1045 $cm^{-1}$ were ascribed to the stretch vibration of C=O, unsaturated carbon, and C-O of ether, respectively (Fei et al., 2020). The increase in the intensity of these bands indicated that the lignin in the WGH powder was decomposed during the drying process (Li et al., 2020). It could be seen that PVD and SMIR damage the molecular structure of WGH powder the most and HPD the least.

### *3.5. bioactive substances of WGH analysis*

Fig. 4A shows the content of bioactive components in the WGHE by different drying methods. The order of TPC was TH-HAD> SD> HPD> SMIR> PVD, and the lowest TPC (6.58 mg/g) was found for PVD samples, which was contrary to the results of Geng et al (2023). This may be due to the fact that the vacuum pump pumped in fresh air with sufficient oxygen content during the atmospheric pressure of drying, which intensified the oxidative decomposition of phenolics. TFC of the PVD samples was significantly higher than the other dried samples (33.26 mg/g), which may be

due to the fact that the vacuum pump takes away a large amount of water vapor during evacuation, reducing the decomposition of flavonoids (Xu et al., 2021). HPD samples had the lowest TFC (25.59 mg/g), which may be due to the longer drying time and higher humidity in the drying chamber leading to the decomposition of flavonoids. The study by Laeliocattleya et al. (2020) also confirmed the decreasing flavonoid content with the increase of drying time. TTC was in the order of: SD> SMIR> TH-HAD> PVD> HPD, where the TTC value of SD samples (15.05 mg/g) was significantly higher than that of mechanically dried samples, and there was no significant difference between mechanically dried samples, which may be due to the lower drying temperature and milder conditions of SD, which caused less thermal damage to the samples. The difference between SD and artificial drying on QC was small, and the QC range was 7.06-8.57 mg/g. TH-HAD and PVD samples have higher retention of phenolics and flavonoids, while the equipment requires higher energy consumption and economic cost, which is suitable for drying products with high added value.

### *3.6. High-resolution liquid chromatography-mass spectrometry (HRLCMS) analysis*

In the present study, HRLCMS was used for the accurate characterization and quantification of various bioactive substances in WGH (Table 5). The results of quantitative analysis showed that the phenolic compounds in WGH were mainly gallic acid, ellagic acid, chlorogenic acid, protocatechin and cryptochlorogenic acid, and the flavonoids were mainly hyperoside, astragaline and quercitrin. This is different from the results of previous studies and may be related to the variety of walnuts, the type and concentration of solvents and the extraction conditions. One study showed that the use of 40% ethanol significantly increased the content of ferulic acid and rutin content (Cosmulescu et al., 2014). Different drying methods differed significantly on the content of monomeric active substances

in WGH. The SD samples contained higher contents of the main components such as hyperoside, quercitrin, astragaline, ellagic acid, epicatechin, ferulic acid, apigenin and gallic acid. The major flavonoids, hypericin, were reduced by 39.93%, 41.60%, 50.68% and 63.16% in the PVD, SMIR, TH-HAD and HPD samples, respectively, and the major polyphenols, gallic acid, were reduced by 53.09%, 45.33%, 48.81% and 41.44%, respectively. Fig. 5 showed the Clustering Heat Map of these active substance components in WGH under different drying methods. As can be seen from the figure, the upper tree shows the clustering of different samples, and the color shades filled in the middle indicate the level of bioactive substance content in each sample, the darker color indicates the higher relative content. From the clustering above, all samples were divided into two categories: SD and artificial drying. Among the artificial drying PVD, SMIR and TH-HAD are one category. SD and HPD samples have a wider variety of monomeric substances with high content, which are suitable for targeted extraction and enrichment of a specific monomeric compound.

### *3.7. Antioxidant activity analysis*

The antioxidant activities of WGHE after different drying treatments are shown in Fig. 4B. The scavenging ability of WGHE treated with different drying methods for DPPH, ABTS, ·OH radicals and Ferric reducing antioxidant power were in the order of TH-HAD> SD> HPD> SMIR> PVD. The same trend of antioxidant capacity and TPC of the samples under different drying methods could be observed, indicating that there is a dose-effect relationship between the antioxidant capacity and TPC. Ribeiro et al. (2023) showed a strong positive correlation between phenolic components and antioxidant capacity, with phenolics being the main contributors to antioxidant capacity. Principal component analysis (PCA) was used to investigate the effects of different drying methods on the

drying time, SEC, bioactive substance content and antioxidant capacity of WGH. At the same time, the chord diagram (Fig. 6) can show the effects of different drying methods on each index more visually.

### *3.8. Principal component analysis*

The principal component analysis plot is shown in Fig. 7, where the first dimension designed as PC1 explained 56.2% of the total variability, while the second dimension denoted as PC2 explained 23.3% of the total variability. Antioxidant capacity, TPC, TTC and drying time had a greater contribution to PC1, while SEC and TFC showed a greater negative correlation with PC1. As shown in the figure, there was a positive correlation between TPC, TTC and antioxidant activity, and the higher the TPC, the stronger the antioxidant capacity. SEC and drying time show a negative correlation, the longer the drying time the more energy is consumed. The results indicate a better reproducibility within the sample group and a greater similarity between HPD and SMIR.

## 4 Conclusions

In this study, the effects of different drying methods on the drying characteristics, physical properties, active substance content and antioxidant capacity of WGH were investigated. The results showed that different drying methods had significant effects on the color of WGH ( $\Delta E > 5$). The time of artificial drying was much lower than that of SD, which greatly improved the drying rate, with the shortest drying time in SMIR. Notably, the specific energy consumption required for HPD were significantly lower than those of other artificial drying methods. HPD samples showed better hydration properties and microstructure. The active substance content of SD, PVD and TH-HAD

samples was higher and the antioxidant capacity of TH-HAD, SD and HPD samples was higher. The retention rate of monomeric active substances in the samples was higher for SD and HPD. Since WGH is a kind of agricultural waste with high yield and low cost, it is important to reduce its economic cost while also improving its product quality as much as possible. Therefore, considering both energy consumption and product quality, HPD is a WGH drying method with industrial potential application due to its low equipment cost, low energy consumption and simple operation.

## Acknowledgments

We gratefully acknowledge the financial support from the National Key R&D Program of China (2019YFD1002404).

## Conflict of Interest Statement

The authors declare that they have no known competing financial interests or personal relationships that could have appeared to influence the work reported in this paper.

## References

Adenitan, AA., Awoyale, W., Akinwande, BA., Busie, MD., & Michael, S. (2021). Mycotoxin profiles of solar tent-dried and open sun-dried plantain chips. Food Control, 119, 107467. https://doi.org/10.1016/j.foodcont.2020.107467.

An, KJ., Fu, MQ., Zhang, H., Tang, DB., Xu, YJ., & Xiao GS. (2019). Effect of ethyl oleate pretreatment on blueberry (Vaccinium corymbosum L.): drying kinetics, antioxidant activity, and structure of wax layer. Journal of food science and technology, 56, 783–791. https://doi.org/10.1007/s13197-018-3538-7.

Asgari, K., Labbafi, M., Khodaiyan, F., Kazemi, M., & Hosseini, SS. (2020). High-methylated pectin from walnut processing wastes

as a potential resource: Ultrasound assisted extraction and physicochemical, structural and functional analysis. International Journal of Biological Macromolecules, 152, 1274–1282. https://doi.org/10.1016/j.ijbiomac.2019.10.224.

Benseddik, A., Azzi, A., Zidoune, MN., & Allaf, K. (2018). Mathematical empirical models of thin-layer airflow drying kinetics of pumpkin slice. Engineering in Agriculture, Environment and Food, 11, 220–231. https://doi.org/10.1016/j.eaef.2018.07.003.

Bettaieb, RI., Bourgou, S., Ben, KS., Aidi, WW., Ksouri, R., Saidani, TM., & Fauconnier, ML. (2020). On the effect of initial drying techniques on essential oil composition, phenolic compound and antioxidant properties of anise (Pimpinella anisum L.) seeds. Food Measure, 14, 220–228. https://doi.org/10.1007/s11694-019-00284-4.

Cosmulescu, S., Trandafir, I., Nour, V., Ionica, M., & Tutulescu, F. (2014). Phenolics Content, Antioxidant Activity and Color of Green Walnut Extracts for Preparing Walnut Liquor. Notulae Botanicae Horti Agrobotanici Cluj-Napoca, 42, 551–555. https://doi.org/10.15835/nbha4229649.

Deli, M., Petit, J., Nguimbou, RM., Beaudelaire, DE., Njintang, YN., & Scher, J. (2019). Effect of sieved fractionation on the physical, flow and hydration properties of Boscia senegalensis Lam., Dichostachys glomerata Forssk. and Hibiscus sabdariffa L. powders. Food science and biotechnology, 28, 1375–1389. https://doi.org/10.1007/s10068-019-00597-6.

Deng, L., Mujumdar, AS., Yang, W., Zhang, Q., Zheng, Z., Wu, M., & Xiao, H. (2020). Hot air impingement drying kinetics and quality attributes of orange peel. Journal of Food Processing and Preservation, 44, 14294. 10.1111/jfpp.14294.

Deng, LZ., Pan, Z., Mujumdar, AS., Zhao, JH., Zheng, ZA., Gao, ZJ., & Xiao, HW. (2019). High-humidity hot air impingement blanching (HHAIB) enhances drying quality of apricots by inactivating the enzymes, reducing drying time and altering cellular structure. Food Control, 96, 104–111. https://doi.org/10.1016/j.foodcont.2018.09.008.

FAO. Statistical database. Food and Agriculture Organization (2020). https://www.fao.org/faostat/en/#data/QCL Accessed 16 December 2022.

Fei, X., Jia, W., Wang, J., Chen, T., & Ling, Y. (2020). Study on enzymatic hydrolysis efficiency and physicochemical properties of cellulose and lignocellulose after pretreatment with electron beam irradiation. International Journal of Biological Macromolecules,

145, 733-739. https://doi.org/10.1016/j.ijbiomac.2019.12.232.

Geng, Z., Zhu, L., Wang, J., Yu, X., Li, M., Yang, W., Hu, B., Zhang, Q., & Yang, X. (2023). Drying sea buckthorn berries (Hippophae rhamnoides L.): Effects of different drying methods on drying kinetics, physicochemical properties, and microstructure. Frontiers in Nutrition, 10, 1106009-1106009. https://doi.org/10.3389/FNUT.2023.1106009.

Hu, Y., Que, T., Fang, Z., Liu, W., Chen, S., Liu, D., & Ye, X. (2013). Effect of Different Drying Methods on the Protein and Product Quality of Hairtail Fish Meat Gel. Drying Technology 31, 1707–1714. https://doi.org/10.1080/07373937.2013.794831.

Ismail, O., Seyhun, KA., & Doymaz, I. (2019). Drying of Okra by Different Drying Methods: Comparison of Drying time, Product Color Quality, Energy Consumption and Rehydration. ATHENS JOURNAL OF SCIENCES, 6, 155–168. https://doi.org/10.30958/ajs.6-3-1.

Jiang, L., Wang, F., Xie, X., Xie, C., Li, A., Xia, N., Gong, X., & Zhang, H. (2022). Development and characterization of chitosan/guar gum active packaging containing walnut green husk extract and its application on fresh-cut apple preservation. International Journal of Biological Macromolecules, 209, 1307–1318. https://doi.org/10.1016/j.ijbiomac.2022.04.145.

Laeliocattleya, RA., Martati, E., Alwi, NS., Aulia, LP., & Yunianta. (2020). The characteristics of corn silk (Zea mays L.) herbal drinks tea with vacuum drying method as antioxidant. IOP Conference Series: Earth and Environmental Science, 475, 012023. https://doi.org/ 10.1088/1755-1315/475/1/012023.

Li, T., Wang, L., Chen, Z., Li, C., Li, X., & Sun, D. (2020). Structural changes and enzymatic hydrolysis yield of rice bran fiber under electron beam irradiation. Food and Bioproducts Processing, 122, 004. https://doi.org/10.1016/j.fbp.2020.04.004.

Liu, X., Wu, Y., Lu, Y., Liu, XW., Liu, J., Ren, J., Wu, W., Wang, Y., & Li, J. (2022). Enhanced effects of walnut green husk solution on the phytoextraction of soil Cd and Zn and corresponding microbial responses. Chemosphere, 289, 133136. https://doi.org/ 10.1016/J.CHEMOSPHERE.2021.133136.

Lugo, L., Ureña, Núñez., & Barrera, Díaz. (2017). Gamma irradiated orange peel for Cr (VI) bioreduction. Separation Science and Technology, 52, 2443-2455. https://doi.org/ 10.1080/01496395.2017.1302477.

Mozaffari, P., Pashangeh, S., Berizi, E., Majlesi, M., Hosseinzadeh, S., Salehi, S.O., Derakhshan, Z., & Giannakis, S. (2022). Potential of nanochitosan coating combined with walnut green husk to improve the preservation of rainbow trout (Oncorhynchus mykiss) during refrigerated storage. Environmental Research, 214, 114019. https://doi.org/10.1016/j.envres.2022.114019.

Namsanguan, Y., Tia, W., Devahastin, S., & Soponronnarit, S. (2004). Drying Kinetics and Quality of Shrimp Undergoing Different Two-Stage Drying Processes. Drying Technology, 22, 759–778. https://doi.org/10.1081/DRT-120034261.

Nguyen, VT., Van, VQ., Bowyer, MC., Van, A., & Scarlett, CJ. (2015). Effects of Different Drying Methods on Bioactive Compound Yield and Antioxidant Capacity of Phyllanthus amarus. J. Drying Technology, 33, 1006–1017. https://doi.org/10.1080/07373937.2015.1013197.

Onwude, DI., Hashim, N., Abdan, K., Janius, R., & Chen, G. (2018). Investigating the influence of novel drying methods on sweet potato (Ipomoea batatas L.): Kinetics, energy consumption, color, and microstructure. Journal of food process engineering, 41, 12686. https://doi.org/10.1111/jfpe.12686.

Ozsoy, N., Can, A., Yanardag, R., & Akev, N. (2008). Antioxidant activity of Smilax excelsa L. leaf extracts. J. Food Chemistry, 110, 571–583. https://doi.org/10.1016/j.foodchem.2008.02.037.

Qin, D., Xiang, B., Zhou, X., Qiu, S., Xi, J., (2022). Microemulsion as solvent for naphthoquinones extraction from walnut (Juglans mandshurica Maxim) green husk using high voltage electrical discharge. Separation and Purification Technology, 281, 119983. https://doi.org/10.1016/J.SEPPUR.2021.119983.

Romano, R., Aiello, A., Meca, G., De, LL., Pizzolongo, F., & Masi P. (2021). Recovery of bioactive compounds from walnut (Juglans regia L.) green husk by supercritical carbon dioxide extraction. International Journal of Food Science & Technology, 56, 4658–4668. https://doi.org/10.1111/IJFS.15161.

Ribeiro, Jéssica., Barros, H., Macedo, VE., Gualberto, S., Silva, Andréa., Souza, C., Zanuto, Márcia., & Silva, M. (2023). Composition, Antinutrients and Antioxidant Capacity of Genipap (Genipa americana;L): Activity of Phenolic Constituents on the Thermal Stability of β-carotene. Journal of Culinary Science & Technology, 21, 215-237. https://doi.org/ 10.1080/15428052.2021.1914263.

Senadeera, A., Önal, DM., & Russo. (2020). Influence of Different Hot Air Drying Temperatures on Drying Kinetics, Shrinkage, and Colour of Persimmon Slices Foods, 9, 101-101. https://doi.org/10.3390/foods9010101.

Shen, HY., Hou, YJ., Xi, MH., Cai, YY., Ao, JF., Wang, J., Li, M., & Luo, AW. (2022). Electron beam irradiation enhanced extraction and antioxidant activity of active compounds in green walnut husk. Food Chemistry, 373, 131520. https://doi.org/10.1016/j.foodchem.2021.131520.

Singh, S., Agrawal, N., Habou, D., Asere, AA., Alhassan, AM., Eklou, AS., Ines, MS., & Francis, N. (2021). Effect of drying methods on the nutritional content and In-vitro Antioxidant capacity of Chenopodium album L. and Spinacia oleracea L. Research Journal of Pharmacy and Technology, 14, 4361-4366. https://doi.org/ 10.52711/0974-360X.2021.00757.

Sarkar, T. (2021). Drying kinetics, fouruer-transform infrared spectroscopy analysis and sensory evaluation of sun, hot-air, microwave and freeze-dried mango leather. JOURNAL OF MICROBIOLOGY BIOTECHNOLOGY AND FOOD SCIENCES 10, 3313. https://doi.org/10.15414/jmbfs.3313.

Seerangurayar, T., Abdulrahim, M., AlIsmaili., Janitha, J., & Nasser, A. (2019). Effect of solar drying methods on color kinetics and texture of dates. Food and Bioproducts Processing, 116, 227-239. https://doi.org/10.1016/j.fbp.2019.03.012.

Tayyab, RM., Liu, K., Ahmed, JM., Safdar, B., Lv, D., & Wei, D. (2022). Developing ultrasound-assisted hot-air and infrared drying technology for sweet potatoes. Ultrasonics Sonochemistry, 86, 106047. https://doi.org/10.1016/j.ultsonch.2022.106047.

Tu, J., Liu, H., Sun, N., Liu, S., & Chen, P. (2018). Optimization of the Steam Explosion Pretreatment Effect on Total Flavonoids Content and Antioxidative Activity of Seabuckthom Pomace by Response Surface Methodology. Molecules, 24, 60. https://doi.org/10.3390/molecules24010060.

Tunckal, C., & Doymaz, İ. (2020). Performance analysis and mathematical modelling of banana slices in a heat pump drying system. Renewable Energy, 150, 918–923. https://doi.org/ 10.1016/j.renene.2020.01.040.

Xiang, J., Li, W., Ndolo, V.U., Beta, T., (2019). A comparative study of the phenolic compounds and in vitro antioxidant capacity of finger millets from different growing regions in Malawi. Journal of Cereal Science, 87, 143–149. https://doi.org/

10.1016/j.jcs.2019.03.016.

Xie, L., Mujumdar, AS., Fang, XM., Wang, J., Dai, JW., Du, ZL., Xiao, HW., Liu, Y., & Gao ZJ. (2017). Far-infrared radiation heating assisted pulsed vacuum drying (FIR-PVD) of wolfberry (Lycium barbarum L.): Effects on drying kinetics and quality attributes. Food and Bioproducts Processing, 102, 320–331. https://doi.org/10.1080/07373937.2020.1818254.

Xu, P., Peng, X., Yang, J., Li, X., Zhang, H., Jia, X., Liu, Y., Wang, Z., & Zhang, Z. (2021). Effect of vacuum drying and pulsed vacuum drying on drying kinetics and quality of bitter orange (Citrus aurantium L.) slices. Food Process, 45, 16098. https://doi.org/10.1111/jfpp.16098.

Xu, Y., Xiao, Y., Lagnika, C., Li, D., Liu, C., Jiang, N., Song, J., & Zhang, M. (2020). A comparative evaluation of nutritional properties, antioxidant capacity and physical characteristics of cabbage (Brassica oleracea var. Capitate var L.) subjected to different drying methods. Food Chemistry, 309, 124935. https://doi.org/10.1016/j.foodchem.2019.06.002.

Zhang, Q., Li, S., Zhang, M., Mu, G., Li, X., Zhang, G., & Xiong, S. (2022). Heat Pump Drying of Kelp (Laminaria japonica): Drying Kinetics and Thermodynamic Properties. Processes, 10, 514. https://doi.org/10.3390/PR10030514.

Zheng, X., Wang, J., Liu, X., Sun, Y., Zheng, Y., Wang, X., & Liu, Y. (2015). Effect of hydrolysis time on the physicochemical and functional properties of corn glutelin by Protamex hydrolysis. Food Chemistry, 172, 407–415. https://doi.org/ 10.1016/j.foodchem.2014.09.080.

# Figures

**Fig. 1.**

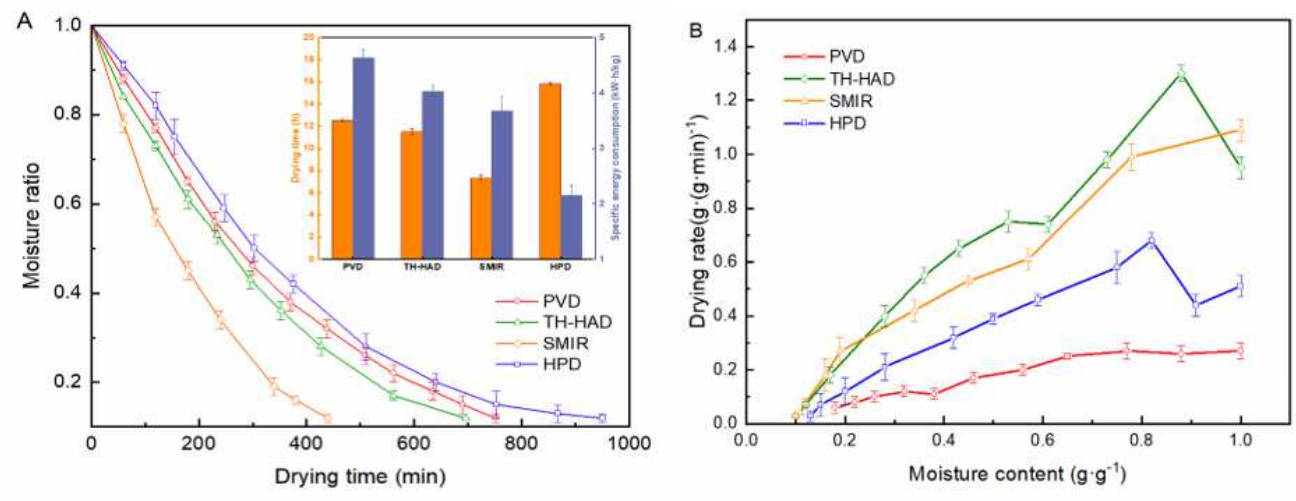


**Figure 1**

Drying curve (A) and drying rate curve (B) of walnut green husk with different drying methods.

**Fig. 2.**

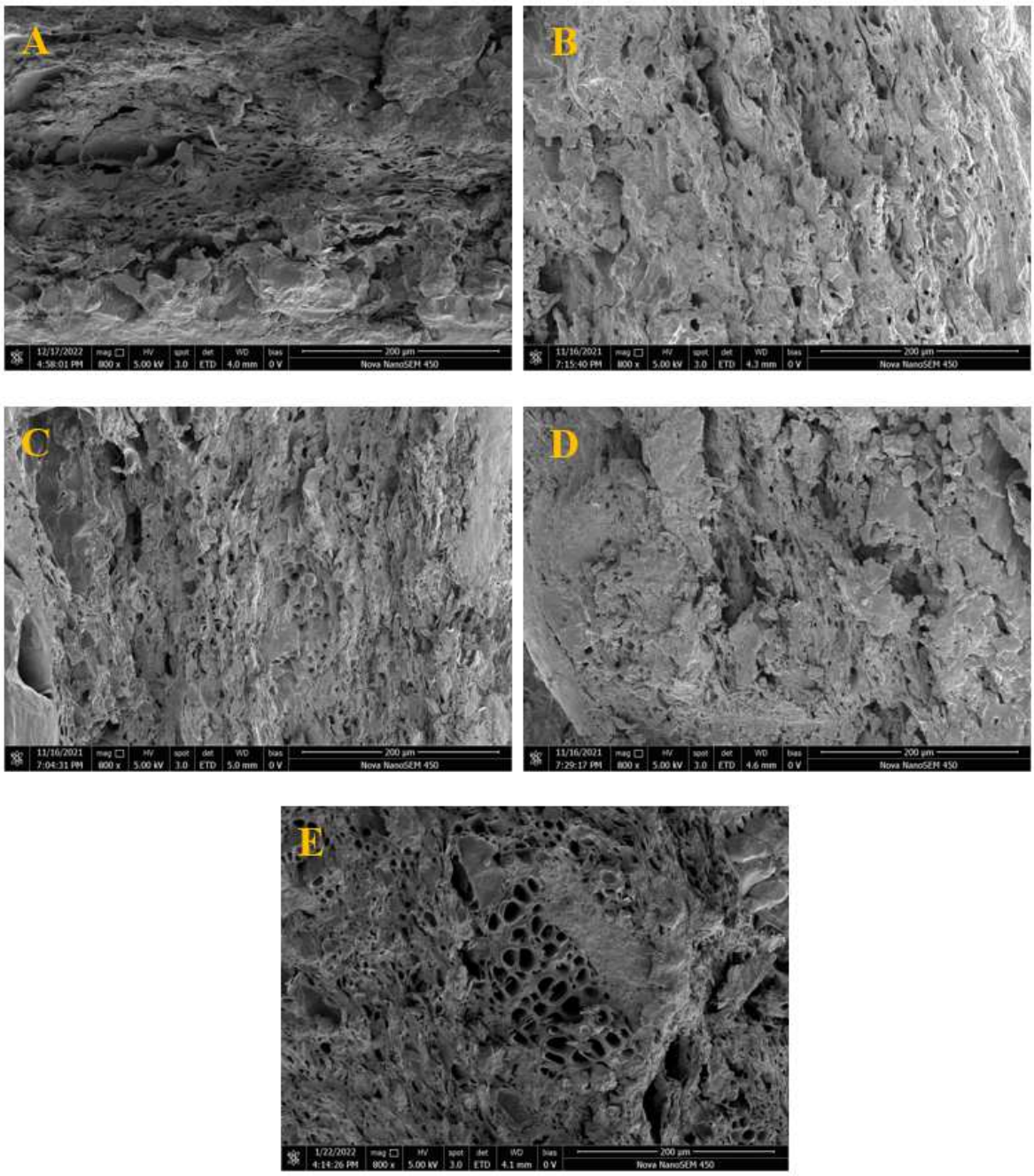


## Figure 2

The Microstructure images by scanning electron of walnut green husk cross section during different drying methods. Magnification is 800×. A: sun drying; B: pulsed vacuum drying; C: short and medium infrared radiation drying; D: hot air drying based on temperature and humidity control; E: heat pump drying.

**Fig. 3.**

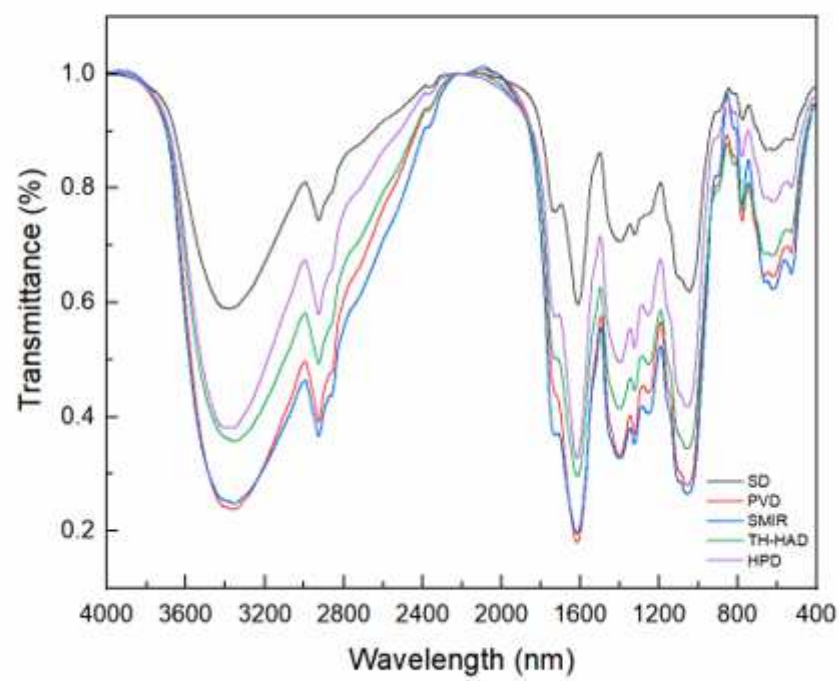


## Figure 3

Fourier transform infrared spectra of walnut green husk during different drying methods.

**Fig. 4.**

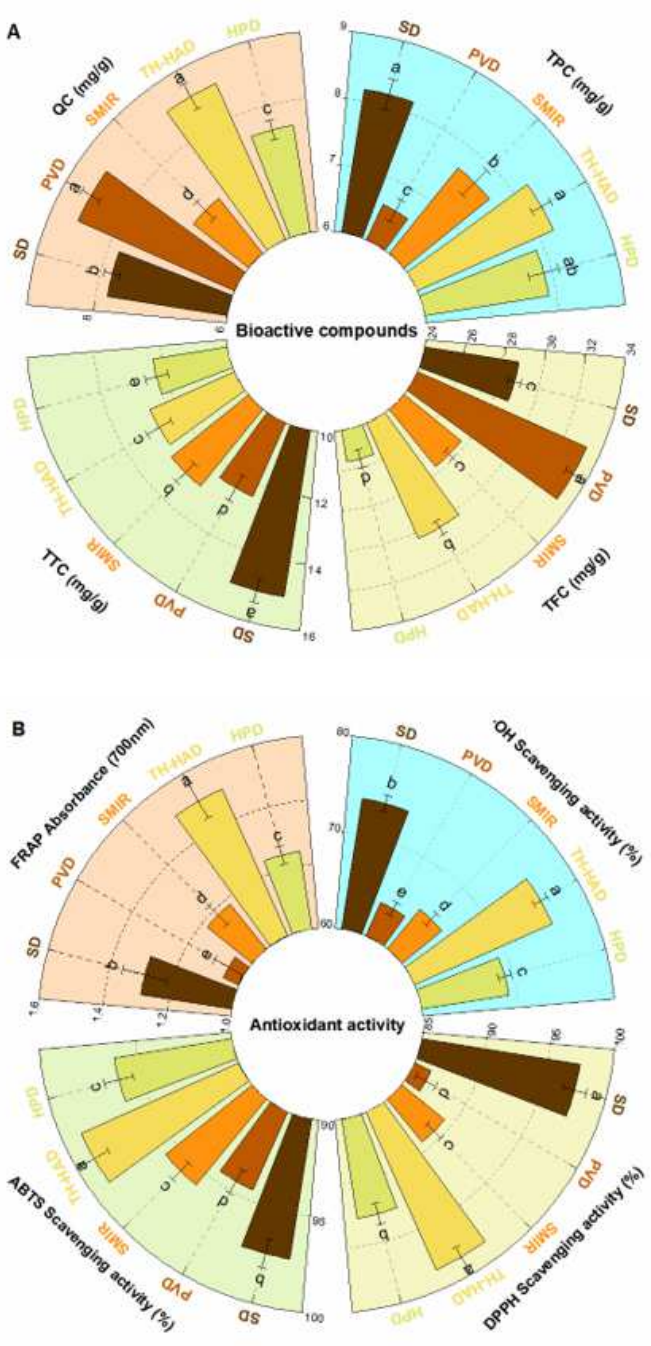


## Figure 4

Effects of different drying methods on the content of bioactive compounds in WGHE (A). The Antioxidant characteristics of WGHE under different drying methods (B). TTC: total terpenoid content; TPC: total phenolic content; TFC: total flavonoid content; QC: quinone content; SD: sun drying; PVD: pulsed vacuum drying; SMIR: short and medium infrared radiation drying; TH-HAD: hot air drying based on temperature and humidity control; HPD: heat pump drying.

**Fig. 5.**

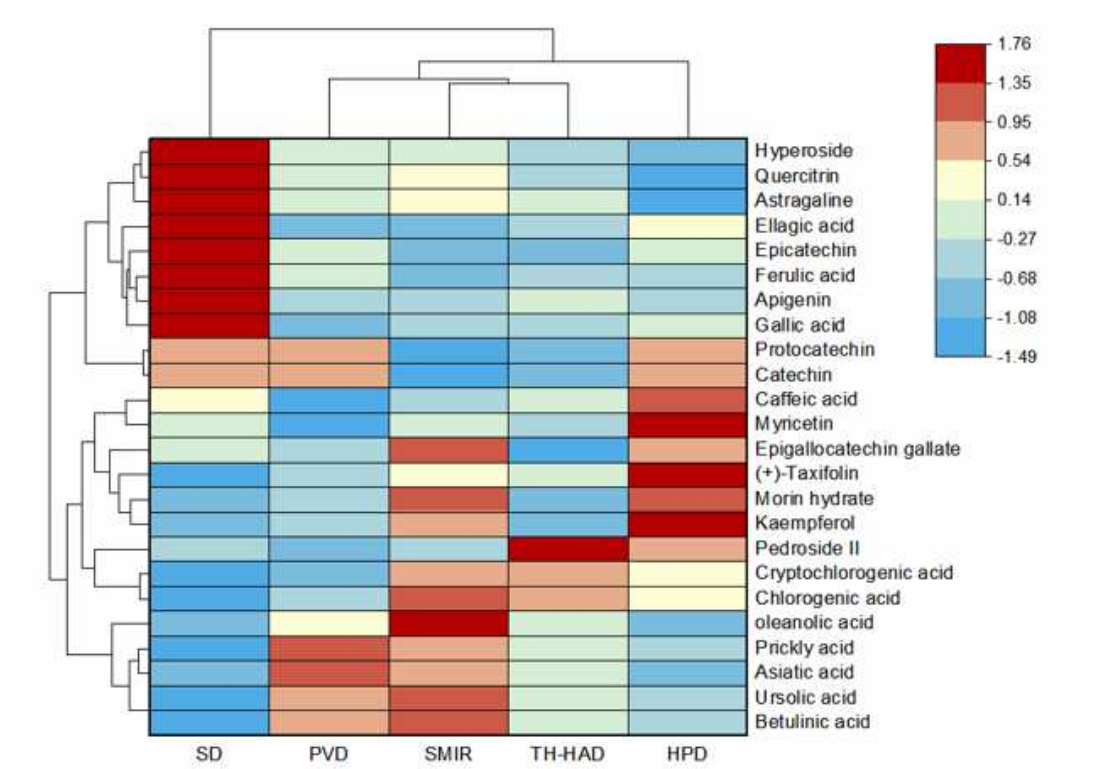


## Figure 5

Clustering Heat Map analysis of various active substances of walnut husk in different drying methods.

**Fig. 6.**

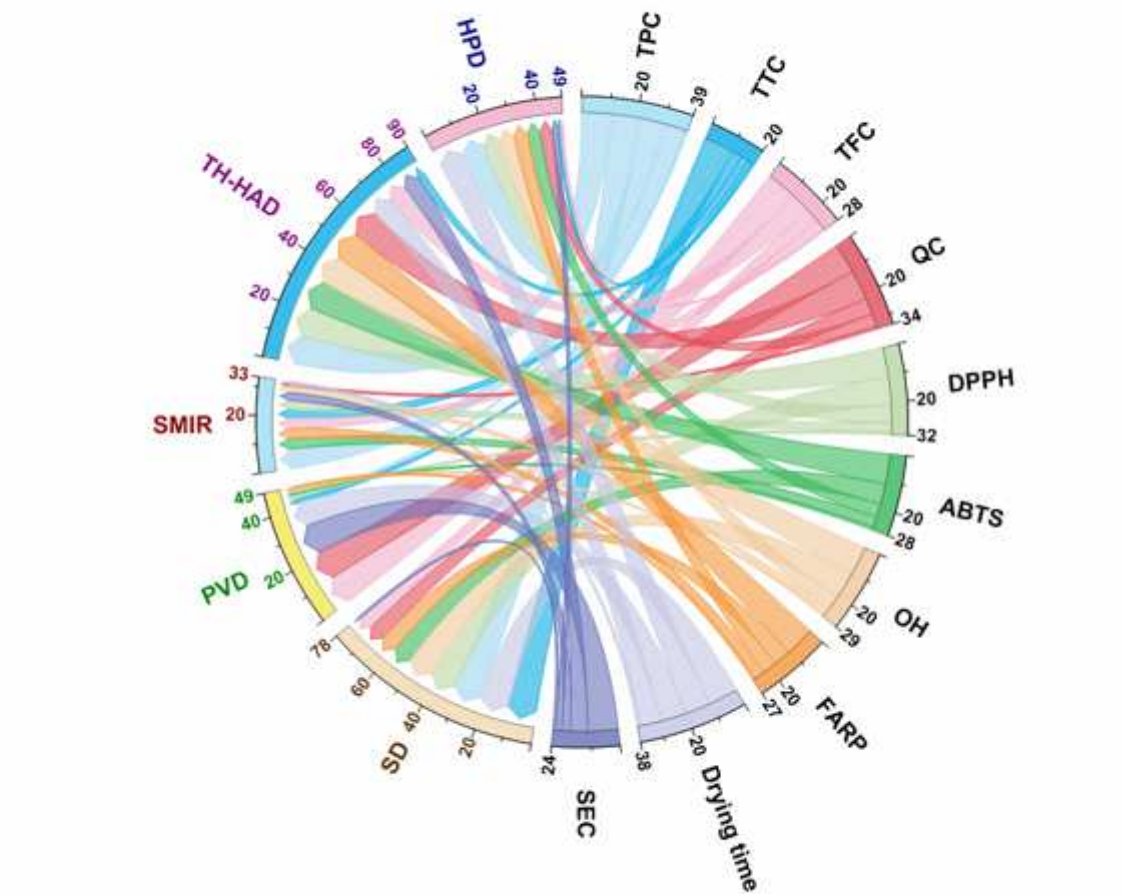


## Figure 6

Chord diagram of relationship between drying method and indexes of walnut green husk. Abbreviation: SD: sun drying; PVD: pulsed vacuum drying; SMIR: short and medium infrared radiation drying; TH-HAD: hot air drying based on temperature and humidity control; HPD: heat pump drying; TTC: total terpenoid content; TPC: total phenolic content; TFC: total flavonoid content; QC: quinone content; SEC: specific energy consumption.

Fig. 7.

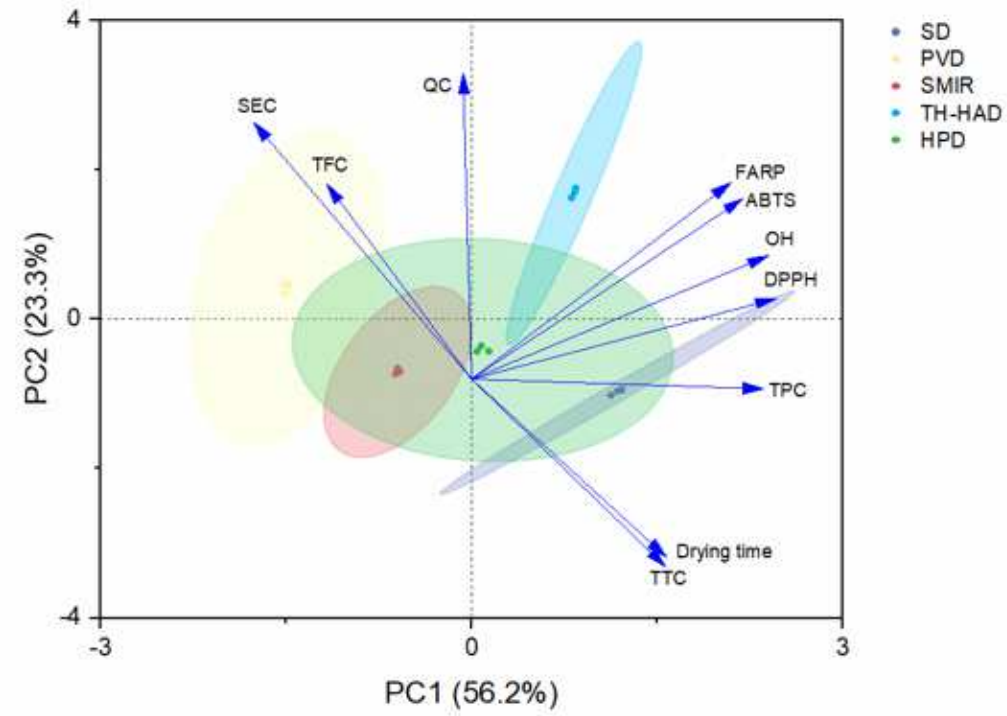


**Figure 7**

Principal component analysis (PCA) biplot for bioactive substances, antioxidant activity and dry characteristics of dried walnut green husk.

## Supplementary Files

This is a list of supplementary files associated with this preprint. Click to download.

- GraphicalAbstract.png